

# Leveraging Multi-facet Paths for Heterogeneous Graph Representation Learning

Jong Woo Kim  
 Korea Advanced Institute of Science and Technology (KAIST)  
 South Korea  
 gsds4885@kaist.ac.kr

Bryan Wong  
 Korea Advanced Institute of Science and Technology (KAIST)  
 South Korea  
 bryan.wong@kaist.ac.kr

Seong Yeub Chu  
 Korea Advanced Institute of Science and Technology (KAIST)  
 South Korea  
 chseye7@kaist.ac.kr

Hyung Min Park  
 Korea Advanced Institute of Science and Technology (KAIST)  
 South Korea  
 mike980406@kaist.ac.kr

Mun Yong Yi\*  
 Korea Advanced Institute of Science and Technology (KAIST)  
 South Korea  
 munyi@kaist.ac.kr

## Abstract

Recent advancements in heterogeneous GNNs have enabled significant progress in embedding nodes and learning relationships across diverse tasks. However, traditional methods rely heavily on meta-paths grounded in node types, which often fail to encapsulate the full complexity of node interactions, leading to inconsistent performance and elevated computational demands. To address these challenges, we introduce MF2Vec, a novel framework that shifts focus from rigid node-type dependencies to dynamically exploring shared facets across nodes, regardless of type. MF2Vec constructs multi-faceted paths and forms homogeneous networks to learn node embeddings more effectively. Through extensive experiments, we demonstrate that MF2Vec achieves superior performance in node classification, link prediction, and node clustering tasks, surpassing existing baselines. Furthermore, it exhibits reduced performance variability due to meta-path dependencies and achieves faster training convergence. These results highlight its capability to analyze complex networks comprehensively. The implementation of MF2Vec is publicly available at <https://anonymous.4open.science/r/MF2Vec-6ABC>.

## CCS Concepts

- Do Not Use This Code → Generate the Correct Terms for Your Paper; Generate the Correct Terms for Your Paper; Generate the Correct Terms for Your Paper; Generate the Correct Terms for Your Paper.

\*Corresponding author.

Permission to make digital or hard copies of all or part of this work for personal or classroom use is granted without fee provided that copies are not made or distributed for profit or commercial advantage and that copies bear this notice and the full citation on the first page. Copyrights for components of this work owned by others than the author(s) must be honored. Abstracting with credit is permitted. To copy otherwise, or republish, to post on servers or to redistribute to lists, requires prior specific permission and/or a fee. Request permissions from permissions@acm.org.

Conference'17, July 2017, Washington, DC, USA

© Copyright held by the owner/author(s). Publication rights licensed to ACM. ACM ISBN 978-x-xxxx-xxxx-x/YY/MM  
<https://doi.org/XXXXXXX.XXXXXXX>

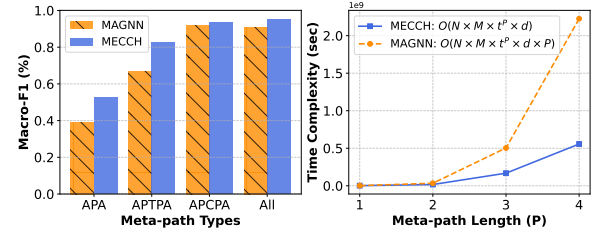


**Figure 1: Performance and time complexity of MECCH and MAGNN on the DBLP dataset.** The left chart shows Macro-F1 instability across meta-path types (APA, APTPA, APCPA, All), highlighting sensitivity to meta-path selection. The right chart illustrates exponential time complexity growth with meta-path length ( $P$ ) due to diverse intermediate node combinations. Notations:  $N$  = nodes,  $M$  = meta-paths,  $t$  = average neighbors,  $P$  = meta-path length,  $d$  = embedding dimension.

## ACM Reference Format:

Jong Woo Kim, Seong Yeub Chu, Hyung Min Park, Bryan Wong, and Mun Yong Yi. . Leveraging Multi-facet Paths for Heterogeneous Graph Representation Learning. In . ACM, New York, NY, USA, 12 pages. <https://doi.org/XXXXXXX.XXXXXXX>

## 1 Introduction

Graph Neural Networks (GNNs) have emerged as powerful tools for capturing complex structures and relationships within graph data, with applications spanning numerous domains [11, 16, 24]. As a specialized branch of GNNs, Heterogeneous Graph Neural Networks (HGNNs) [8–10, 15, 25] aim to address the unique challenges of modeling graphs with diverse types of nodes and edges by introducing tailored mechanisms for efficient learning. Among these, relation-based HGNNs enhance learning by aggregating messages along edges categorized by relation types, yet they often encounter limitations due to the deep network structures required to process multi-hop relations, leading to over-smoothing and diminished performance [8].

To mitigate these challenges, meta-path-based HGNNs leverage meta-paths to construct homogeneous subgraphs, reducing the

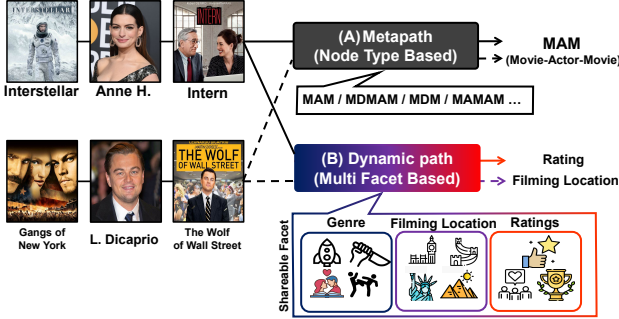


**Figure 2: Comparison of schema assignment for IMDB data. (A) Existing methods use predefined schemas based on node types. (B) The proposed approach dynamically assigns paths using multi-facet criteria, selecting the most descriptive facet, such as filming location, genre, or rating.**

need for multi-hop message passing. For instance, the “MAM” meta-path on the IMDB dataset links Movie and Actor nodes, capturing collaborative relationships between movies via shared actors [8, 9, 26]. Despite their efficiency, such meta-path-based approaches are constrained by rigid node-type combinations, which give rise to several critical limitations.

First, meta-paths can only reflect specific relationships between certain types of nodes, which limits their ability to capture a wide range of relationships in a detailed manner. For example, the “MAM” meta-path captures collaborations between movies that share the same actor but fails to represent more detailed relationships beyond it such as sharing genres or countries. Second, as depicted in Figure 1 (left), the performance of meta-path-based models fluctuates depending on the selected meta-path, resulting in instability across datasets and tasks [13, 22]. Third, as shown in Figure 1 (right), the exponential increase in meta-path combinations and lengths with diverse intermediate nodes amplifies computational costs and exploration complexity. Even with advanced learnable meta-path approaches like GTN [27] and MHNF [22], these issues persist due to their reliance on fixed node-type configurations.

This paper introduces a novel Multi-Facet Path approach to address these limitations. The concept of a facet, representing distinct attributes or properties of nodes (e.g., filming location or production year for a movie), is expanded from prior works on homogeneous graphs [3, 18, 21] to encompass shared characteristics across diverse node types in heterogeneous graphs. By shifting from node-type-based paths to facet-based constructions, the proposed method offers a flexible and granular modeling framework that overcomes the rigidity and inefficiency of traditional meta-path approaches.

Through dynamic facet embeddings, which are learned and updated in an end-to-end manner, the Multi-Facet Path approach enables the representation of intricate relationships across nodes, enhancing both efficiency and model stability. First, the use of facets allows for the capture of a broader range of relationships, enriching downstream task representations. Second, this method minimizes performance variability by dynamically constructing paths based on facet information rather than fixed meta-paths. Third, the elimination of manual meta-path definitions and the reduction of computational overhead further bolster scalability.

Figure 2 demonstrates that even when following the same meta-path, nodes can be grouped based on different facets. For example, the paths “New York-L. Dicaprio-The Wolf of Wall Street” and “Interstellar-Anne H.-Intern” may simply be grouped as “Movie-Actor-Movie” under meta-path-based methods. However, with a multi-facet approach, the path “New York-L. Dicaprio-The Wolf of Wall Street” can be considered from the perspective of filming location, while the path “Interstellar-Anne H.-Intern” may reflect similarities in IMDb ratings. This approach allows the model to comprehensively capture latent and rich information within the graph, effectively overcoming the limitations of traditional meta-path-based methods.

In MF2Vec, paths are extracted from the adjacency matrix of a heterogeneous graph through random walks without distinguishing them by predefined meta-path types. The node embeddings of the extracted paths are projected into a shared facet space of  $K$  dimensions. Gumbel Softmax and an attention mechanism are employed to select the most relevant facets for intermediate nodes, ensuring a discrete yet differentiable selection process. These facets characterize the relationships between endpoint nodes and compute path weights that reflect their importance for node connections. Finally, a homogeneous network is constructed by integrating same-typed nodes and fed into a Graph Convolutional Network (GCN) [16], which aggregates multi-facet vectors along the paths to generate latent node representations. Key contributions of this work are summarized as follows:

- **Dynamic Facet Embedding:** A novel framework for constructing flexible paths independent of node types.
- **Efficiency and Performance Enhancement:** Reduction in computational costs and enhanced performance for node classification, node clustering, and link prediction tasks
- **Stable Performance:** Significant improvement in stability across datasets and tasks by mitigating dependence on fixed meta-paths.

## 2 Related Work

### 2.1 Heterogeneous Graph Neural Network (HGNN)

Graph neural networks (GNNs) effectively handle graph-structured data by learning low-dimensional node representations [4, 11, 16, 24]. Building on GNNs, heterogeneous graph neural networks (HGNNs) extend representation learning to heterogeneous graphs, enabling tasks like node classification, link prediction, and clustering. Message-passing methods have become prominent, generating embeddings by aggregating neighbor information.

**2.1.1 Relation-based HGNNs.** Relation-based HGNNs aggregate neighbor information with type-specific weights, eliminating manual meta-path definitions. RGAT [2] applies relation-specific GCNs, while RGAT [1] integrates self-attention for relational interactions. HetSANN [12] and HGT [13] use meta-relation-based attention, and Simple-HGN [19] combines type-level and node-level attention with L2 normalization. While efficient, deeper layers may cause over-smoothing [17] and performance degradation.

**2.1.2 Metapath-based HGNNs.** Metapath-based HGNNs analyze complex networks using predefined metapaths, enabling direct

links between homogeneous nodes. Metapath2vec [5] uses random walks with a skip-gram model [20], while HAN [25] and MAGNN [9] aggregate features along metapaths. GTN [27] dynamically learns metapaths, and GraphHINGE [15] efficiently aggregates interactions. Models like HeCo [26], HMSG [10], MHNF [22], and MECCH [8] enhance robustness and reduce redundancy. Despite progress, most approaches rely on single-facet paths, limiting their granularity. To address this, MF2Vec introduces a multi-faceted, fine-grained approach for richer node interactions and network understanding.

## 2.2 Multiple-Vector Network Embedding

Recent studies in graph representation learning focus on learning multiple embeddings for nodes, capturing their multi-faceted nature. PolyDW [18] uses matrix factorization-based clustering to assign facet distributions, independently sampling facets for target and context nodes. Splitter [6] generates multi-facet node embeddings aligned with the original representation. Asp2vec [21] introduces a differentiable facet selection module and regularization to explore interactions across facets. For multi-relational graphs, r-GAT [3] aggregates relation-specific neighborhood information and applies query-aware attention to select relevant facets. However, existing methods are limited to single-node facets in homogeneous graphs. We extend these approaches to heterogeneous graphs by transforming meta-path schemas into diverse facets, linking terminal node facets for richer interaction understanding.

## 3 Preliminary

This section provides definitions of terminologies used in the current study. The notations and their explanations are summarized in Table 1.

**Definition 1 (Heterogeneous Graph).** A heterogeneous graph  $G = (V, \mathcal{E})$  is characterized by a node type mapping function  $\phi : V \rightarrow \mathcal{A}$  and an edge type mapping function  $\psi : \mathcal{E} \rightarrow \mathcal{R}$ , where  $\mathcal{A}$  and  $\mathcal{R}$  are sets of node and edge types, respectively, with  $|\mathcal{A}| + |\mathcal{R}| > 2$ .

**Definition 2 (Metapath).** A metapath is a sequence  $A_1 \xrightarrow{R_1} A_2 \xrightarrow{R_2} \dots \xrightarrow{R_k} A_{k+1}$  (or  $A_1 A_2 \dots A_{k+1}$ ), representing a composite relation  $R = R_1 \circ R_2 \circ \dots \circ R_k$  between node types  $A_1$  and  $A_{k+1}$ .

**Definition 3 (Metapath Schema).** A metapath schema is a sequence of node types  $A_1, A_2, \dots, A_{k+1}$  connected by edge types  $R_1, R_2, \dots, R_k$ . This schema represents the structural pattern of a metapath and illustrates how different node types are related through specific types of relationships defined by the nodes and edges.

**Definition 4 (Multi-facet Node Representation Learning).** For a graph  $G = (V, \mathcal{E})$  with nodes  $V$ , the goal is to learn a multi-facet node embedding  $E_{facet}(v_i) \in \mathbb{R}^{K \times d}$  for each node  $v_i$ . Here,  $K$  is the number of facets, and each facet embedding  $E_n(v_i) \in \mathbb{R}^{1 \times d}$  aims to: 1) preserve network structure, 2) capture various facets of  $v_i$ , and 3) represent facet interactions.

**Definition 5 (Multi-facet Path).** Unlike predefined metapaths, a multi-facet path  $P = v_1 \xrightarrow{R_1} v_2 \xrightarrow{R_2} \dots \xrightarrow{R_m} v_{m+1}$  is extracted without manual specification. Intermediate nodes  $v_2, \dots, v_m$  are

projected onto multi-facet vectors  $F_2, \dots, F_m$ , forming a multi-facet path  $P = v_1 \rightarrow F_2 \rightarrow \dots \rightarrow F_m \rightarrow v_{m+1}$ . This path integrates information from intermediate nodes through multiple facets, updating node representations based on various latent information beyond node types.

## 4 Methodology

In this section, we describe our approach, as shown in Figure 3. We begin by extracting paths between homogeneous end nodes using random walks, similar to traditional metapath methods [5, 7]. We then project the features of intermediate nodes into multiple facets and aggregate these facets to create multi-facet embedding representations. These representations are used as edge features between path-guided neighbors and the target node. The model pseudocode is provided in Algorithm 1, and the notations are summarized in Table 1.

### Algorithm 1 MF2Vec Forward Propagation

---

**Input:** The heterogeneous graph  $G = (V, \mathcal{E})$ ; The target embedding matrix  $E_n(V') \in \mathbb{R}^{|V'| \times d}$   
**Output:** Final node embeddings  $h^L(V')$   
**Define:**  $v_s$  represents the intermediate node of the path  $path(v_i, v_j)$

```

while not convergence do
     $L_{warm-up}(v_i) \leftarrow run\_warm-up(v_i)$ 
     $L_{warm-up}(V') = \sum_{i=1}^{|V|} L_{warm-up}(v_i)$ 
    Update  $E(V')$  by minimizing  $L_{warm-up}$ 
end while
Perform a sub-graph  $G' = (V', \mathcal{E}')$  through Random Walk between certain type nodes
Function Run Our Model  $(V')$ 
for each  $v_i \in V'$  do
     $E_{facet}(v_i) = \{E_n(v_i)\}_{n=1}^k = W_1 \cdot E(v_i)$ , where  $W_1 \in \mathbb{R}^{d \times d}$ 
     $P_{facet}(v_i, v_j) = \{P_n(v_i, v_j)\}_{n=1}^k = \text{Agg}(E_{facet}(v_s))$ 
     $P(v_i, v_j) = \sum_{n=1}^k \sigma(W_2 \cdot P_n(v_i, v_j)) \cdot P_n(v_i, v_j)$ , where  $W_2 \in \mathbb{R}^{1 \times d}$ 
end for
for each  $l = 1, \dots, L$  do
    for each  $v_i \in V'$  do
         $h^{l+1}(v_i) = \sigma \left( \text{BN} \left( \sum_{j \in N(i)} P(v_i, v_j) \cdot h^l(v_j) \right) \right)$ 
    end for
end for
return  $h^L(v_i)$ 

```

---

Table 1: Notations and Explanations

Notation	Explanation
$\mathbb{R}^d$	$d$ -dimensional Euclidean space
$G = (V, \mathcal{E})$	A heterogeneous graph with a node set $V$ and an edge set $\mathcal{E}$
$G' = (V', \mathcal{E}')$	A subgraph with a certain node type set $V'$ and a certain node type edge set $\mathcal{E}'$
$v_i$	A node $v_i \in V'$
$E(v_i)$	The embedding of node $v_i$
$E_n(v_i)$	$n$ -th multi-facet embedding of node $v_i$
$E_{facet}(v_i)$	Multi-facet embedding of node $v_i$
$h^L(v_i)$	Final embedding of node $v_i$ after $L$ -th layer
$path(v_i, v_j)$	The set of whole nodes in the path between node $v_i$ and $v_j$
$path_{inter}(v_i, v_j)$	Intermediate nodes in the path between node $v_i$ and $v_j$
$P(v_i, v_j)$	The embedding of the path between node $v_i$ and $v_j$
$P_n(v_i, v_j)$	$n$ -th multi-facet embedding of the path between node $v_i$ and $v_j$
$P_{facet}(v_i, v_j)$	Multi-facet embedding of the path between node $v_i$ and $v_j$
$\alpha_n^p$	Weight of $n$ -th facet in the path $p$

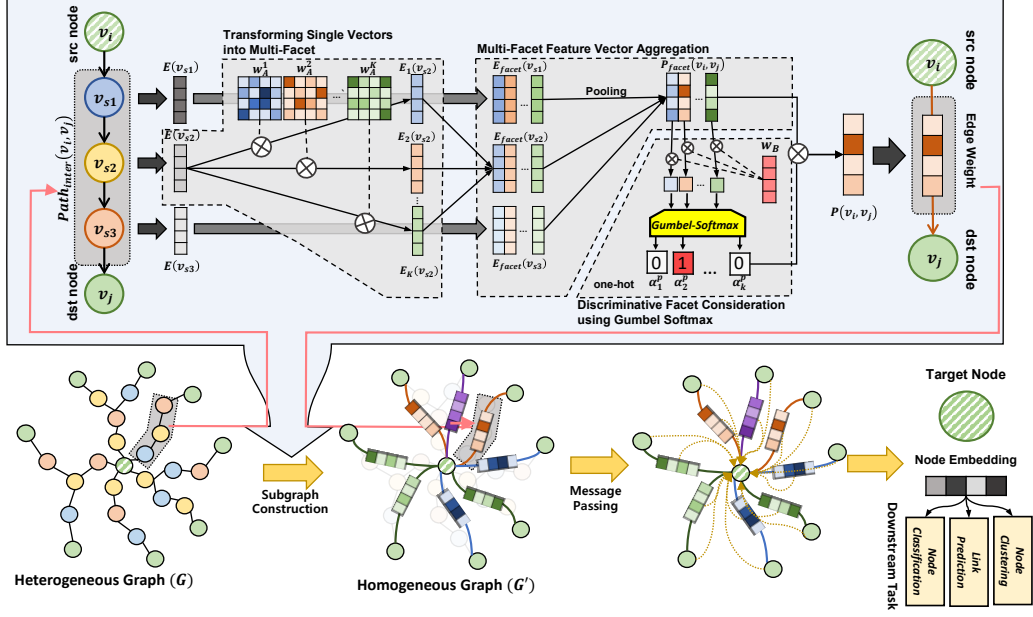


Figure 3: Overall Architecture

#### 4.1 Extracting Paths Using Random Walk

Given a node type  $A$ , our method constructs a homogeneous subgraph that identifies direct connections between nodes of type  $A$ , the same as traditional metapath-based models. Instead of relying on metapath schemas such as APA or APCPA, the method generates a path starting from a node of type  $A$  and applies a random walk, traversing randomly selected adjacent nodes until encountering a type  $A$  node. This approach captures relationships within a specified path length limit, effectively mapping connections within the nodes of a type without being constrained by predefined metapath patterns. Details of the *Random Walk* algorithm are provided in Algorithm 2.

#### 4.2 Transforming Single Embeddings into Multi-Facet

Our model captures inherent information from all node types before generating a facet embedding. Initially, node information is exchanged through a GNN warm-up phase, which facilitates the aggregation of neighborhood information and enriches the initial node embeddings with structural and semantic context. The node embedding,  $E(v_i)$ , is defined during this warm-up phase and serves as the foundation for training the main model. The resulting node embedding  $E(v_i)$  is then refined into a multi-dimensional embedding  $E_{\text{facet}}(v_i)$  to capture diverse information, as detailed in Equation 1.

$$E_n(v_i) = W_A^n E(v_i), \quad n \in \{1, 2, \dots, K\}$$

$$E_{\text{facet}}(v_i) = [E_1(v_i) \parallel E_2(v_i) \parallel \dots \parallel E_K(v_i)] \quad (1)$$

Here,  $E_n(v_i)$  represents the multi-facet embedding of node  $v_i$  within the  $n$ -th facet, where  $W_A^n$  is the corresponding weight matrix with dimensions  $d \times d$  for the  $n$ -th facet, and  $K$  represents

the total number of facets. The individual facet embeddings are subsequently concatenated into a unified multi-facet embedding,  $E_{\text{facet}}(v_i)$ , providing a comprehensive representation.

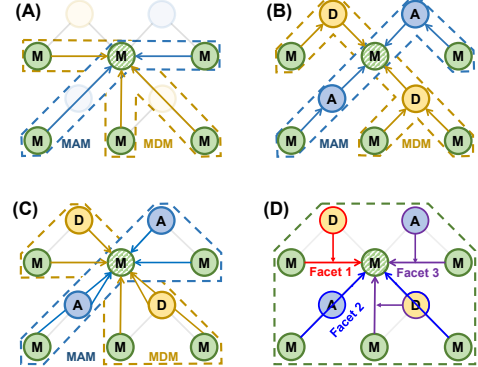


Figure 4: HGNN aggregation for the dashed green target node.  $M$ ,  $D$ , and  $A$  denote node types. Approaches: (a) HAN: connection between metapath-based neighbors by ignoring intermediate nodes instance based on node path schemas. (b) MAGNN & MHNF: connection between metapaths including intermediate nodes. (c) MECCH: all nodes are directly connected per metapath for contextual representation. (d) MF2Vec: multi-facet neighbors connected with facet-based edge features without using metapath connections.

### 4.3 Multi-facet Feature embedding Aggregation

To construct a multi-facet feature embedding for paths consisting of multiple nodes, we employ an aggregation function that synthesizes information from the nodes along the path. The mathematical formulation for this aggregation is given by Equation 2.

$$P_{\text{facet}}(v_i, v_j) = f(E_{\text{facet}}(v_s) \mid v_s \in \text{path}_{\text{inter}}(v_i, v_j)) \quad (2)$$

In the given equation,  $P_{\text{facet}}(v_i, v_j)$  represents the aggregated multi-facet feature embedding for a connection between nodes  $v_i$  and  $v_j$ . The set  $\text{path}_{\text{inter}}(v_i, v_j)$  consists of intermediate nodes between  $v_i$  and  $v_j$ , and  $v_s$  is an intermediate node within the path. The function  $f$  signifies an aggregation operation using mean pooling.

### 4.4 Discriminative Facet Consideration using Gumbel Softmax

We utilize the Gumbel Softmax [14] function to introduce randomness and uncertainty into facet selection, which helps the model explore diverse facet influences in complex relationships. The temperature parameter  $\tau$  allows us to control the balance between exploration and exploitation. This approach enables us to capture nuanced facet interactions and dependencies, making our model more adaptable and robust for multi-facet data. Even if the random walk algorithm extracts the paths that are little related to the end nodes, we mitigate their impact by assigning higher weights to the most crucial components using Gumbel softmax. As a result, we effectively operate within constrained environments, even without extracting meaningful paths.

$$\begin{aligned} \alpha_n^p &= \sigma(W_B P_n(v_i, v_j)) \\ P(v_i, v_j) &= \sum_{n=1}^K \alpha_n^p \cdot P_n(v_i, v_j) \end{aligned} \quad (3)$$

In the given equation,  $\sigma$  represents Gumbel Softmax.  $P(v_i, v_j)$  is the final embedding for  $\text{path}(v_i, v_j)$  that combines these probabilities and  $W_B$  is a matrix with dimensions  $1 \times d$ .

### 4.5 Subgraph Construction

Path-based HGNNs transform the input graph into a new homogeneous subgraph  $G^P = (V^P, \mathcal{E}^P)$  for each node and path, where  $G^P$  varies by model. For example, in HAN,  $G^P$  represents the metapath- $P$ -guided neighborhood, while MAGNN defines it as instances of metapath- $P$  incident to the node. MECCH constructs subgraphs using most metapaths as illustrated in Figure 4.

Our approach, however, avoids the need for multiple metapaths by leveraging multi-facet information from a single path between nodes. This results in a subgraph  $G' = (V', \mathcal{E}')$  that provides richer information than traditional methods. The MF2Vec model efficiently learns complex node relationships by constructing subgraphs as described in Algorithm 3 incorporating multi-dimensional edge features which are multi-facet embedding for a more comprehensive node representation.

### 4.6 Message Passing

To extract node embeddings, we utilize GCN. In this process, we consider interactions between nodes and utilize path facets as edge features. The formula for calculating graph node embeddings is as

**Table 2: Statistics of Datasets. NC: Node Classification, LP: Link Prediction, CL: Node Clustering.**

Dataset	# Nodes (# Types)	# Edges	Target (# Labels)	Task
Yelp	31,081 (3)	411,263	User-Business	LP
MovieLens	2,672 (4)	234,695	User-Movie	LP
DBLP	26,128 (4)	119,783	Author (4)	NC, CL
ACM	11,246 (3)	17,426	Paper (3)	NC, CL
IMDB	11,519 (3)	17,009	Movie (3)	NC, CL
Freebase	43,854 (4)	75,517	Movie (3)	NC, CL

follows:

$$h^{(l+1)}(v_i) = \sigma \left( \text{BN} \left( \sum_{j \in N(i)} P(v_i, v_j) \cdot h^l(v_j) \right) \right) \quad (4)$$

In this equation,  $\sigma$  represents the activation function, which is ELU, and BN represents the batch normalization. The  $P(v_i, v_j)$  denotes the path facet feature between node  $i$  and its neighbor  $j$ , which is utilized as an edge feature.

### 4.7 Training Losses

We train our model for two tasks: node classification and link prediction. For node classification, the cross-entropy loss  $L_{nc}$  is computed over labeled nodes  $V_L$ , measuring the disparity between true labels  $y_v$  and predictions  $y'_v$ :

$$L_{nc} = - \sum_{v \in V_L} y_v \log(y'_v).$$

For link prediction, where node labels are unavailable, we minimize the contrastive loss  $L_{lp}$  using positive  $V^+$  and negative  $V^-$  node pairs:

$$L_{lp} = - \sum_{(v, \text{pos}) \in V^+} \log(\sigma(h_v^T h_{\text{pos}})) - \sum_{(v, \text{neg}) \in V^-} \log(\sigma(-h_v^T h_{\text{neg}})).$$

Here,  $\sigma(\cdot)$  is the sigmoid function, ensuring effective learning for link prediction.

## 5 Experiment

In this part, we assess the performance and practicality of our introduced method through tests on link prediction, node classification, and node clustering tasks across five diverse graph datasets. The primary goals of these experiments are to address the following research questions.

- RQ1. How well does MF2Vec perform on downstream tasks?
- RQ2. How stable is the performance of MF2Vec in downstream tasks?
- RQ3. How time-efficient is MF2Vec?

### 5.1 Experimental Settings

**5.1.1 Datasets.** We evaluate our model on six heterogeneous graph datasets: DBLP, ACM, IMDB, and Freebase for node classification and clustering, and Yelp and MovieLens for link prediction. Experiments include 1000 trials per node with a walk length of 5, covering typical metapaths (e.g., APA, APCPA) using consistent data splits. Dataset details are summarized in Table 2.

**5.1.2 Baselines.** We compare MF2Vec against state-of-the-art heterogeneous graph neural networks (HGNNs), categorized as follows: (a) Relation-Based HGNNs, including RGCN, RGAT, HGT,

HetSANN, and Simple-HGN; and (b) Metapath-Based HGNNs, comprising MP2Vec, HAN, MAGNN, HeCo, MHNF, HGMAE HMSG, and MECCH.

**5.1.3 Graph Construction Settings.** Following Algorithm 2, we ensured that the node types matched the target node and that the path length was at most 5. For each target node, we performed up to 1000 trials. The number of negative samples was set to 1.

**5.1.4 Experimental Settings.** To ensure a fair comparison among all heterogeneous graph neural networks (HGNNs), the node embedding dimension was fixed to 64. The learning rate was set to  $1 \times 10^{-3}$ , weight decay to  $1 \times 10^{-5}$ , and the dropout rate to 0.5. For each baseline model, hyperparameters such as batch size, attention heads, dropout rate, learning rate, and epochs—excluding the node embedding dimension—followed the default settings specified in the original papers. Training was conducted using the Adam optimizer with early stopping (patience of 20 epochs) to prevent overfitting. Specifically, for MF2Vec, the temperature ( $\tau$ ) was set to 0.5, and the number of facets ( $K$ ) was set to 5. To demonstrate generalization, the experiments were conducted using five seed values (1, 10, 100, 1000, and 10000), with the data split into train (80%), validation (10%), and test (10%). The model seeds were fixed during the experiments, and the average and standard deviation of the results were calculated for all seeds.

## 5.2 Downstream Task (RQ1)

**5.2.1 Node Classification.** In our node classification experiments, we convert nodes into low-dimensional vector embeddings and apply a Softmax function to obtain probability distributions over label categories. We evaluate the model using Micro-F1, Macro-F1, and AUC metrics, providing a balanced assessment of classification performance. These metrics are used to compare our model, MF2Vec, against baseline models on the DBLP, ACM, IMDB and Freebase datasets, with results presented in Table 3.

Our approach consistently outperforms baseline models across all metrics, demonstrating the effectiveness of MF2Vec. The significant performance improvement, particularly on the IMDB dataset, highlights the model’s ability to capture complex relational data through multi-facet vectors. This suggests that MF2Vec effectively reveals nuanced relationships within heterogeneous information networks (HINs), enhancing understanding beyond node types.

**5.2.2 Link Prediction.** In MovieLens and Yelp, link prediction is framed as a binary classification task to determine the presence of an edge in the original graph. During training, validation, and testing, negative edges are created by replacing the destination node in positive edges with a randomly chosen node that is not connected to the source node. The link probability is computed using the dot product of node embeddings:  $p_{v_a, v_b} = \sigma(v_a^T \cdot v_b)$ , where  $\sigma$  is the sigmoid function.

Table 4 presents the AUC, Micro-F1, and Macro-F1 scores for our model and baselines on Yelp and MovieLens. MF2Vec performs competitively on Yelp (against MECCH) and outperforms all baselines on MovieLens. These results highlight the advantage of using multi-facet vectors derived from node paths for link prediction, and demonstrate the efficacy of our model in updating embeddings without relying on node types.

**5.2.3 Node Clustering.** We carry out node clustering experiments using the DBLP, ACM, IMDB, and Freebase datasets to assess the embedding quality produced by MF2Vec. In these experiments, similar to node classification, we utilize the embedding vectors of target nodes from the testing set as input for the K-Means model and employ NMI and ARI metrics to gauge performance. As presented in Table 5, our model surpasses the baseline models, except for MHNF [22] in ARI on the IMDB dataset, where MF2Vec closely follows it by a small margin, demonstrating our model’s superior ability to generate effective node representations based on multi-facet vectors for node clustering.

## 5.3 Stability of performance (RQ2)

This section emphasizes the stability advantage of leveraging multi-facets from paths in our model. Unlike metapath-based models that depend on predefined schemas (e.g., APA, APCPA), MF2Vec achieves consistent performance across different schema types, effectively capturing fine-grained information regardless of metapath type. To validate this, we compare single-metapath performance across all models, including MF2Vec, on the DBLP, ACM, and IMDB datasets.

Table 6 presents the standard deviations in node classification performance using a single metapath. While other models show significant performance variation depending on the chosen metapath, MF2Vec demonstrates remarkable stability. For the DBLP dataset, performance variations highlight the reliance of metapath-based models on predefined paths and the associated time and cost of analysis, which MF2Vec effectively mitigates.

## 5.4 Time Complexity (RQ3)

The proposed model’s time complexity is  $O(N \times K \times t \times d)$ , where  $N$  is the number of nodes,  $t$  is the average neighbors,  $K$  is the number of facets, and  $d$  is the embedding dimension. Attention adds  $O(N \times t \times K \times d)$ , and graph convolution contributes  $O(N \times t \times d)$ , resulting in a total complexity of  $O(N \times K \times t \times d)$ .

In Table 7, models like MECCH [8], HAN [25], and MAGNN [9] rely on  $M$  metapaths, incurring higher costs due to  $t^P$  growth with metapath length ( $P$ ). MF2Vec avoids this by leveraging facets ( $K$ ), leading to more efficient computation, satisfying  $MF2Vec < MECCH \approx HAN < MAGNN$ . Additionally, we compare MF2Vec with relation-based methods like HetSANN [12] and SimpleHGN [19], which also avoid metapaths by focusing on edge types.

Figure 5 compares training times (log scale) and Macro F1 scores for MF2Vec and other models on DBLP, IMDB, and MovieLens. MAGNN [9] and MP2Vec [5] are excluded from MovieLens due to their excessive training times. MF2Vec achieves the best performance on node classification and link prediction tasks, with significantly lower training times. This efficiency arises from its dynamic use of path characteristics, avoiding the high costs of aggregating multiple paths as seen in MAGNN and MP2Vec, ensuring better scalability and faster convergence without compromising performance.

## 5.5 Visualization

To evaluate embedding quality, we visualize node representations from various HGNNs on the DBLP dataset using t-SNE [23]. Figure

**Table 3: Node classification performance. Best results are in bold, second-best are underlined.**

Dataset		DBLP			ACM			IMDB			Freebase		
Model	AUC	Mi-F1	Ma-F1	AUC	Mi-F1	Ma-F1	AUC	Mi-F1	Ma-F1	AUC	Mi-F1	Ma-F1	
Relation-based	RGCN	<b>0.858<math>\pm</math>0.004</b>	0.842 $\pm$ 0.005	<u>0.837<math>\pm</math>0.005</u>	0.810 $\pm$ 0.012	0.769 $\pm$ 0.007	0.762 $\pm$ 0.011	0.533 $\pm$ 0.024	0.431 $\pm$ 0.027	0.337 $\pm$ 0.043	0.574 $\pm$ 0.049	0.508 $\pm$ 0.057	0.408 $\pm$ 0.078
	RGAT	<b>0.849<math>\pm</math>0.003</b>	0.829 $\pm$ 0.004	<u>0.823<math>\pm</math>0.004</u>	0.803 $\pm$ 0.021	0.761 $\pm$ 0.023	0.749 $\pm$ 0.025	0.558 $\pm$ 0.011	0.424 $\pm$ 0.015	0.409 $\pm$ 0.016	0.622 $\pm$ 0.027	0.553 $\pm$ 0.033	0.487 $\pm$ 0.037
	HGT	0.926 $\pm$ 0.017	0.889 $\pm$ 0.026	0.899 $\pm$ 0.022	0.779 $\pm$ 0.016	0.741 $\pm$ 0.016	0.709 $\pm$ 0.024	0.540 $\pm$ 0.019	0.396 $\pm$ 0.024	0.386 $\pm$ 0.022	0.578 $\pm$ 0.030	0.482 $\pm$ 0.034	0.427 $\pm$ 0.037
	HetSANN	0.950 $\pm$ 0.006	0.931 $\pm$ 0.007	0.925 $\pm$ 0.008	0.780 $\pm$ 0.023	0.736 $\pm$ 0.025	0.711 $\pm$ 0.027	0.613 $\pm$ 0.006	0.487 $\pm$ 0.010	0.484 $\pm$ 0.007	0.646 $\pm$ 0.021	0.575 $\pm$ 0.027	0.521 $\pm$ 0.030
	Simple-HGN	0.947 $\pm$ 0.011	0.928 $\pm$ 0.011	0.920 $\pm$ 0.015	0.840 $\pm$ 0.037	0.808 $\pm$ 0.033	0.793 $\pm$ 0.045	0.612 $\pm$ 0.035	0.497 $\pm$ 0.038	0.481 $\pm$ 0.045	0.671 $\pm$ 0.014	0.630 $\pm$ 0.017	0.548 $\pm$ 0.031
Metapath-based	MP2Vec	0.586 $\pm$ 0.020	0.399 $\pm$ 0.025	0.372 $\pm$ 0.026	0.731 $\pm$ 0.010	0.663 $\pm$ 0.010	0.633 $\pm$ 0.014	0.511 $\pm$ 0.011	0.397 $\pm$ 0.016	0.378 $\pm$ 0.013	0.605 $\pm$ 0.019	0.603 $\pm$ 0.022	0.506 $\pm$ 0.030
	HAN	0.937 $\pm$ 0.003	0.919 $\pm$ 0.003	0.909 $\pm$ 0.004	0.785 $\pm$ 0.011	0.762 $\pm$ 0.009	0.729 $\pm$ 0.014	0.550 $\pm$ 0.020	0.426 $\pm$ 0.021	0.384 $\pm$ 0.034	0.665 $\pm$ 0.011	0.643 $\pm$ 0.014	0.517 $\pm$ 0.033
	MAGNN	0.972 $\pm$ 0.003	0.926 $\pm$ 0.003	0.915 $\pm$ 0.003	0.945 $\pm$ 0.014	0.806 $\pm$ 0.031	0.777 $\pm$ 0.049	0.739 $\pm$ 0.013	0.534 $\pm$ 0.032	0.492 $\pm$ 0.070	0.744 $\pm$ 0.015	0.674 $\pm$ 0.019	0.518 $\pm$ 0.063
	HeCo	0.978 $\pm$ 0.003	0.894 $\pm$ 0.013	0.886 $\pm$ 0.014	0.831 $\pm$ 0.019	0.745 $\pm$ 0.012	0.703 $\pm$ 0.013	0.544 $\pm$ 0.006	0.385 $\pm$ 0.014	0.360 $\pm$ 0.004	0.753 $\pm$ 0.021	0.652 $\pm$ 0.021	0.515 $\pm$ 0.033
	MHNF	0.925 $\pm$ 0.004	0.896 $\pm$ 0.006	0.886 $\pm$ 0.006	0.883 $\pm$ 0.009	0.760 $\pm$ 0.012	0.711 $\pm$ 0.016	0.530 $\pm$ 0.042	0.408 $\pm$ 0.042	0.324 $\pm$ 0.071	0.512 $\pm$ 0.013	0.451 $\pm$ 0.014	0.265 $\pm$ 0.053
	HGMAE	0.948 $\pm$ 0.018	0.874 $\pm$ 0.121	0.829 $\pm$ 0.084	0.812 $\pm$ 0.011	0.732 $\pm$ 0.012	0.736 $\pm$ 0.019	0.614 $\pm$ 0.019	0.427 $\pm$ 0.016	0.353 $\pm$ 0.033	0.727 $\pm$ 0.030	0.622 $\pm$ 0.036	0.478 $\pm$ 0.042
	HMSG	0.978 $\pm$ 0.003	0.901 $\pm$ 0.020	0.894 $\pm$ 0.021	0.923 $\pm$ 0.013	0.795 $\pm$ 0.019	0.785 $\pm$ 0.020	0.647 $\pm$ 0.021	0.472 $\pm$ 0.017	0.461 $\pm$ 0.022	0.744 $\pm$ 0.026	0.679 $\pm$ 0.040	0.531 $\pm$ 0.038
	MECCH	0.991 $\pm$ 0.133	0.941 $\pm$ 0.165	0.937 $\pm$ 0.176	0.916 $\pm$ 0.133	0.790 $\pm$ 0.165	0.793 $\pm$ 0.176	0.657 $\pm$ 0.133	0.512 $\pm$ 0.165	0.502 $\pm$ 0.176	0.773 $\pm$ 0.133	0.648 $\pm$ 0.165	0.588 $\pm$ 0.176
<b>MF2Vec</b>		<b>0.991<math>\pm</math>0.002</b>	0.946 $\pm$ 0.011	<u>0.943<math>\pm</math>0.010</u>	<b>0.954<math>\pm</math>0.008</b>	0.843 $\pm$ 0.008	0.837 $\pm$ 0.008	0.768 $\pm$ 0.033	0.603 $\pm$ 0.041	<b>0.581<math>\pm</math>0.052</b>	0.828 $\pm$ 0.023	0.694 $\pm$ 0.021	0.629 $\pm$ 0.047

**Table 4: Link prediction performance. Best results are in bold, second-best are underlined. "-" indicates no data available as MHNF and HGMAE is for node classification.**

Dataset	Yelp			Movielens		
	AUC	Mi-F1	Ma-F1	AUC	Mi-F1	Ma-F1
RGCN	0.635 $\pm$ 0.141	0.621 $\pm$ 0.103	0.614 $\pm$ 0.134	0.741 $\pm$ 0.003	0.664 $\pm$ 0.003	0.664 $\pm$ 0.003
RGAT	0.697 $\pm$ 0.104	0.665 $\pm$ 0.081	0.655 $\pm$ 0.086	0.687 $\pm$ 0.115	0.636 $\pm$ 0.101	0.630 $\pm$ 0.104
HGT	0.832 $\pm$ 0.004	0.771 $\pm$ 0.004	0.770 $\pm$ 0.005	0.755 $\pm$ 0.036	0.711 $\pm$ 0.016	0.711 $\pm$ 0.015
HetSANN	0.703 $\pm$ 0.017	0.689 $\pm$ 0.013	0.688 $\pm$ 0.014	0.774 $\pm$ 0.013	0.772 $\pm$ 0.013	0.771 $\pm$ 0.013
Simple-HGN	0.824 $\pm$ 0.016	0.757 $\pm$ 0.018	0.757 $\pm$ 0.018	0.820 $\pm$ 0.007	0.746 $\pm$ 0.012	0.745 $\pm$ 0.015
MP2Vec	0.718 $\pm$ 0.003	0.658 $\pm$ 0.002	0.664 $\pm$ 0.003	0.798 $\pm$ 0.004	0.662 $\pm$ 0.004	0.669 $\pm$ 0.002
HAN	0.627 $\pm$ 0.102	0.528 $\pm$ 0.076	0.399 $\pm$ 0.140	0.822 $\pm$ 0.004	0.642 $\pm$ 0.050	0.604 $\pm$ 0.072
MAGNN	0.835 $\pm$ 0.005	0.773 $\pm$ 0.002	0.774 $\pm$ 0.003	0.858 $\pm$ 0.010	0.776 $\pm$ 0.008	0.781 $\pm$ 0.009
HeCo	0.838 $\pm$ 0.003	0.767 $\pm$ 0.004	0.755 $\pm$ 0.002	0.839 $\pm$ 0.003	0.755 $\pm$ 0.004	0.771 $\pm$ 0.005
HMSG	0.851 $\pm$ 0.003	0.784 $\pm$ 0.002	0.803 $\pm$ 0.004	0.814 $\pm$ 0.006	0.744 $\pm$ 0.006	0.753 $\pm$ 0.013
MECCH	0.867 $\pm$ 0.012	0.782 $\pm$ 0.013	0.774 $\pm$ 0.015	0.752 $\pm$ 0.006	0.690 $\pm$ 0.015	0.634 $\pm$ 0.040
<b>MF2Vec</b>	<b>0.893<math>\pm</math>0.003</b>	0.820 $\pm$ 0.005	0.824 $\pm$ 0.004	0.918 $\pm$ 0.003	0.840 $\pm$ 0.004	0.847 $\pm$ 0.007

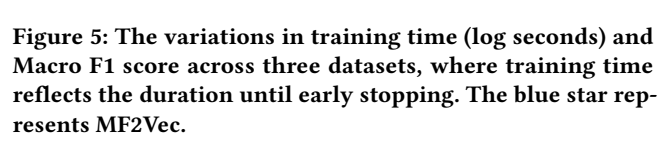
**Table 5: Node clustering performance. Best results are in bold, second-best are underlined. Standard deviations (std) are omitted due to length constraints.**

Dataset	DBLP		ACM		IMDB		Freebase	
	NMI	ARI	NMI	ARI	NMI	ARI	NMI	ARI
RGCN	0.0168	0.0670	0.3612	0.2809	0.0088	0.0056	0.0228	0.0443
RGAT	0.4435	0.4097	0.3976	0.3140	0.0477	0.0143	0.0327	0.0387
HGT	0.7722	0.8250	0.5064	0.5335	0.0433	0.0459	0.0801	0.1075
HetSANN	0.752	0.7723	0.5274	0.5263	0.0865	0.043	0.1054	0.0967
Simple-HGN	0.7707	0.6405	0.5309	0.5237	0.1410	0.1180	0.1541	0.1804
MP2Vec	0.0519	0.0330	0.1034	0.0641	0.0065	0.0096	0.0145	0.0286
HAN	0.3533	0.1845	0.3036	0.3528	0.0057	0.0015	0.0211	0.0217
MAGNN	0.7964	0.8193	0.5125	0.5317	0.1075	0.1199	0.1872	0.1477
HeCo	0.7477	0.7872	0.5394	0.5454	0.0049	0.0028	0.0805	0.0793
MHNF	0.7197	0.7498	0.5385	0.5274	0.1443	<b>0.1467</b>	0.1881	0.1697
HMSG	0.7278	0.7767	0.4475	0.3630	0.0335	0.0326	0.1257	0.1213
MECCH	0.8312	0.8739	0.4202	0.3513	0.0070	0.0056	0.2612	0.3127
<b>MF2Vec</b>	<b>0.8606</b>	<b>0.8951</b>	<b>0.5714</b>	<b>0.5790</b>	<b>0.1459</b>	0.1448	<b>0.3083</b>	<b>0.3729</b>

6 shows t-SNE plots for HAN [25], MAGNN [9], HeCo [26], HMSG [10], MECCH [8], and MF2Vec, with colors representing author classes. MF2Vec demonstrates superior clustering within classes and clear decision boundaries, outperforming the more scattered intra-class distributions and weaker inter-class separations of other HGNNS.

**Table 6: Standard deviation (Std) of node classification performance for single metapaths, comparing the top 3 models and MF2Vec. Lower values (↓) indicate higher stability, with the best and second-best results highlighted.**

Dataset	Metric	MAGNN	HMSG	MECCH	MF2Vec
DBLP	AUC	0.144	0.201	<b>0.118</b>	<b>0.064</b>
	Mi-F1	0.233	0.318	<b>0.195</b>	<b>0.138</b>
	Ma-F1	0.251	0.277	<b>0.197</b>	<b>0.139</b>
ACM	AUC	<b>0.147</b>	0.188	0.211	<b>0.141</b>
	Mi-F1	0.083	0.106	<b>0.076</b>	<b>0.070</b>
	Ma-F1	0.102	0.088	<b>0.066</b>	<b>0.051</b>
IMDB	AUC	0.042	0.041	0.043	<b>0.031</b>
	Mi-F1	<b>0.029</b>	0.049	0.067	<b>0.028</b>
	Ma-F1	0.032	<b>0.030</b>	0.032	<b>0.020</b>

**Table 7: Comparison of Time Complexity. M: Number of metapaths, P: Metapath length,  $t^P$ : Exponential growth of neighbors with P,  $d_{edge}$ : Edge embedding dimension, H: Attention heads.****Figure 5: The variations in training time (log seconds) and Macro F1 score across three datasets, where training time reflects the duration until early stopping. The blue star represents MF2Vec.**

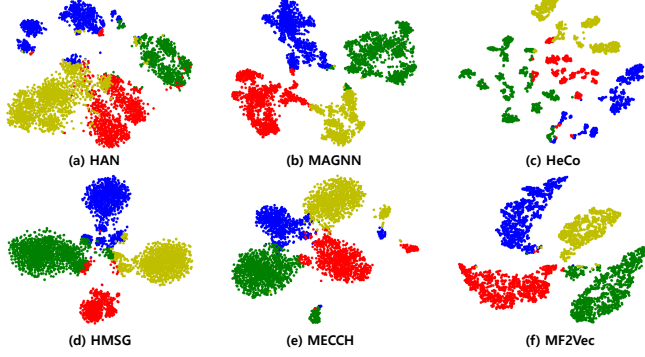


Figure 6: Visualization of the node embedding on DBLP.

## 6 Study of MF2Vec

To analyze the impact of intrinsic characteristics of MF2Vec with respect to various features including train ratio, the number facets, we additionally conducted extensive experiments.

### 6.1 Train Ratio ( $\mathcal{R}$ )

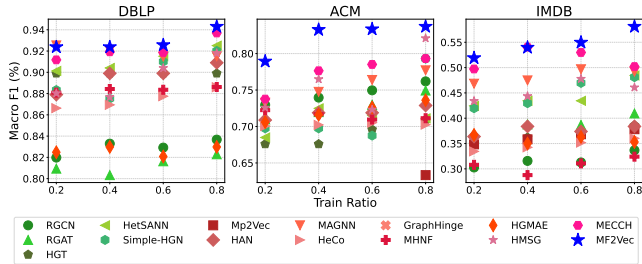


Figure 7: Performance of MF2Vec on three datasets with varying training set ratios, ranging from 0.8 to 0.2, in the node classification task.

As shown in Figure 7, MF2Vec consistently achieves the highest performance across varying training set ratios, demonstrating its robustness and adaptability. While the performance of all models declines as the training ratio decreases, MF2Vec remains its superiority in most cases and retains competitive in the rest. At the lowest ratio of 0.2, it occasionally shows comparable performance to other models. HAN and one baseline were excluded due to significantly lower performance, ensuring clearer visualization. These results highlight MF2Vec's effectiveness in handling sparse training data.

### 6.2 Number of Facets ( $\mathcal{K}$ )

Figure 8 shows MF2Vec's performance across six datasets with varying facet counts. The performance difference relative to " $\mathcal{K} = 1$ " highlights the advantage of multiple facets. Except for IMDB, optimal results are achieved with five facets, consistently outperforming the single-facet case by effectively leveraging node and path information. Beyond five facets, performance declines, likely due to reduced feature grouping efficiency.

### 6.3 Role of Facet Selection

As MF2Vec selects the optimal facet for each path in a learnable manner, we conduct an additional experiment to validate its facet

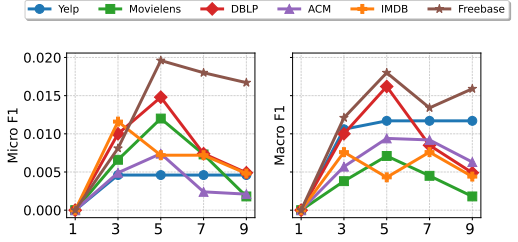


Figure 8: Performance of MF2Vec on six datasets with varying number of facets extracted from a path.

selection strategy. Table 8 compares different methods for selecting facet information as edge weights. Our GCN-based results show that the proposed method, using Gumbel-Softmax and attention mechanisms, outperforms all alternatives across datasets. Random facet selection reduces performance, and omitting facets entirely leads to the lowest results. These findings highlight the importance of facet-related information for effective graph learning and the proposed method's ability to capture complex structures and hidden relationships.

## 7 Case Study

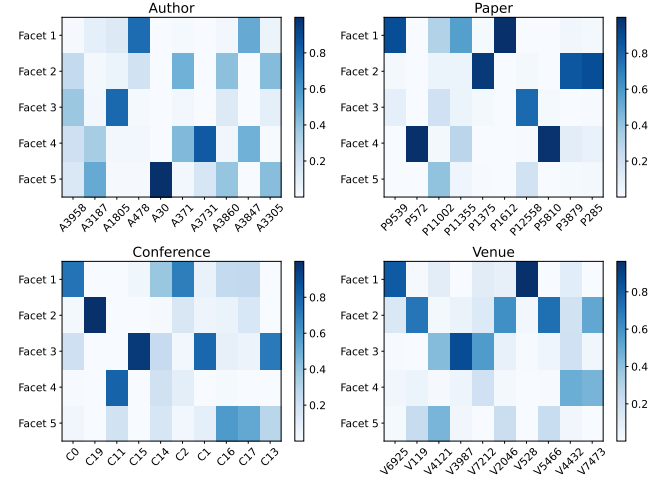


Figure 9: Facet-level attention heatmap for the DBLP dataset. Columns represent 10 sampled nodes per type, and rows indicate shared facets across node types. Darker colors denote facets with greater significance in node connections.

To evaluate facet balance among node types, we analyzed their distribution as shown in Figure 9. The heatmaps reveal equitable attention weights across node types, with each column representing a specific node and highlighting diverse facet distributions. For example, the Paper node "P1612" emphasizes Facet 1, while the Author node "A3958" distributes attention evenly across facets, reflecting varying significance assigned to facets based on connections. This analysis confirms that nodes either focus on specific facets or distribute attention uniformly, with no strong bias toward any facet, validating the importance of modeling shared facets in heterogeneous graphs.

**Table 8: Performance comparison of different methods for reflecting edge weights (Gumble. : Gumble Softmax, Random. : Random Selection, and No. : No Edge Weight) across various datasets. The best results are highlighted in bold, and the second-best results are underlined.**

Dataset	Yelp			Movielens			DBLP			ACM			IMDB			Freebase		
	AUC	Mi-F1	Ma-F1	AUC	Mi-F1	Ma-F1	AUC	Mi-F1	Ma-F1	AUC	Mi-F1	Ma-F1	AUC	Mi-F1	Ma-F1	AUC	Mi-F1	Ma-F1
No.	<u>0.813<math>\pm</math>0.003</u>	0.743 $\pm$ 0.002	0.752 $\pm$ 0.004	<u>0.832<math>\pm</math>0.003</u>	0.754 $\pm$ 0.005	0.743 $\pm$ 0.013	<u>0.974<math>\pm</math>0.004</u>	0.868 $\pm$ 0.012	0.854 $\pm$ 0.012	<u>0.912<math>\pm</math>0.014</u>	0.788 $\pm$ 0.015	0.759 $\pm$ 0.025	<u>0.531<math>\pm</math>0.022</u>	0.378 $\pm$ 0.005	0.232 $\pm$ 0.036	<u>0.731<math>\pm</math>0.011</u>	0.646 $\pm$ 0.021	0.475 $\pm$ 0.015
Random.	<u>0.867<math>\pm</math>0.018</u>	0.797 $\pm$ 0.003	<u>0.808<math>\pm</math>0.015</u>	<u>0.871<math>\pm</math>0.006</u>	0.795 $\pm$ 0.006	0.803 $\pm$ 0.005	<u>0.989<math>\pm</math>0.003</u>	0.935 $\pm$ 0.009	0.931 $\pm$ 0.01	<u>0.949<math>\pm</math>0.009</u>	0.824 $\pm$ 0.013	0.813 $\pm$ 0.012	<u>0.751<math>\pm</math>0.008</u>	0.588 $\pm$ 0.009	0.571 $\pm$ 0.003	<u>0.825<math>\pm</math>0.020</u>	0.696 $\pm$ 0.017	0.628 $\pm$ 0.042
Gumble.	<u>0.893<math>\pm</math>0.003</u>	0.820 $\pm$ 0.005	0.824 $\pm$ 0.004	<u>0.918<math>\pm</math>0.003</u>	0.840 $\pm$ 0.004	0.847 $\pm$ 0.007	<u>0.991<math>\pm</math>0.002</u>	0.946 $\pm$ 0.011	0.943 $\pm$ 0.010	<u>0.954<math>\pm</math>0.008</u>	0.843 $\pm$ 0.008	0.837 $\pm$ 0.008	<u>0.768<math>\pm</math>0.033</u>	0.603 $\pm$ 0.041	0.581 $\pm$ 0.052	<u>0.828<math>\pm</math>0.023</u>	0.694 $\pm$ 0.021	0.629 $\pm$ 0.047

## 8 Conclusion

In this study, we introduce MF2Vec, a novel heterogeneous graph neural network model, which generates node representations using multi-facet vectors from various paths, regardless of node types. MF2Vec captures complex latent semantics through these multi-faceted paths, offering a node-type-agnostic embedding approach. Evaluations across six datasets demonstrate that MF2Vec outperforms leading baseline models in both performance and time complexity. Future work could focus on automating path selection within heterogeneous graph neural networks using learnable methods to improve upon current random pre-selection methods, highlighting the potential of dynamic multi-facet path utilization in graph networks.

## References

- [1] D. Busbridge, D. Sherburn, P. Cavallo, and N. Y. Hammerla. 2019. Relational Graph Attention Networks. *arXiv preprint arXiv:1904.05811* (2019).
- [2] Junjie Chen, Hongxu Hou, Jing Gao, Yatu Ji, and Tiangang Bai. 2019. RGCN: recurrent graph convolutional networks for target-dependent sentiment analysis. In *International Conference on Knowledge Science, Engineering and Management*. Springer, 667–675.
- [3] M. Chen, Y. Zhang, X. Kou, Y. Li, and Y. Zhang. 2021. R-GAT: Relational Graph Attention Network for Multi-Relational Graphs. *arXiv preprint arXiv:2109.05922* (2021).
- [4] Michaël Defferrard, Xavier Bresson, and Pierre Vandergheynst. 2016. Convolutional neural networks on graphs with fast localized spectral filtering. *Advances in neural information processing systems* 29 (2016).
- [5] Yuxiao Dong, Nitesh V Chawla, and Ananthram Swami. 2017. metapath2vec: Scalable representation learning for heterogeneous networks. In *Proceedings of the 23rd ACM SIGKDD international conference on knowledge discovery and data mining*. 135–144.
- [6] Alessandro Epasto and Bryan Perozzi. 2019. Is a single embedding enough? learning node representations that capture multiple social contexts. In *The world wide web conference*. 394–404.
- [7] Tao-yang Fu, Wang-Chien Lee, and Zhen Lei. 2017. Hin2vec: Explore meta-paths in heterogeneous information networks for representation learning. In *Proceedings of the 2017 ACM on Conference on Information and Knowledge Management*. 1797–1806.
- [8] Xinyu Fu and Irwin King. 2024. MECCH: metapath context convolution-based heterogeneous graph neural networks. *Neural Networks* 170 (2024), 266–275.
- [9] Xinyu Fu, Jian Zhang, Ziqiao Meng, and Irwin King. 2020. Magnn: Metapath aggregated graph neural network for heterogeneous graph embedding. In *Proceedings of The Web Conference 2020*. 2331–2341.
- [10] Mengya Guan, Xinjun Cai, Jiaxing Shang, Fei Hao, Dajiang Liu, Xianlong Jiao, and Wancheng Ni. 2023. HMSG: Heterogeneous graph neural network based on Metapath SubGraph learning. *Knowledge-Based Systems* 279 (2023), 110930.
- [11] Will Hamilton, Zhitao Ying, and Jure Leskovec. 2017. Inductive representation learning on large graphs. *Advances in neural information processing systems* 30 (2017).
- [12] Huiting Hong, Hantao Guo, Yucheng Lin, Xiaoqing Yang, Zang Li, and Jieping Ye. 2020. An attention-based graph neural network for heterogeneous structural learning. In *Proceedings of the AAAI conference on artificial intelligence*, Vol. 34. 4132–4139.
- [13] Ziniu Hu, Yuxiao Dong, Kuansan Wang, and Yizhou Sun. 2020. Heterogeneous graph transformer. In *Proceedings of the web conference 2020*. 2704–2710.
- [14] Eric Jang, Shixiang Gu, and Ben Poole. 2016. Categorical reparameterization with gumbel-softmax. *arXiv preprint arXiv:1611.01144* (2016).
- [15] Jiarui Jin, Kounianhua Du, Weinan Zhang, Jiarui Qin, Yuchen Fang, Yong Yu, Zheng Zhang, and Alexander J Smola. 2022. GraphHINGE: Learning Interaction Models of Structured Neighborhood on Heterogeneous Information Network. *ACM Transactions on Information Systems (TOIS)* 40, 3 (2022), 1–35.
- [16] Thomas N Kipf and Max Welling. 2016. Semi-supervised classification with graph convolutional networks. *arXiv preprint arXiv:1609.02907* (2016).
- [17] Q. Li, Z. Han, and X. M. Wu. 2018. Deeper Insights into Graph Convolutional Networks for Semi-Supervised Learning. In *Proceedings of the AAAI Conference on Artificial Intelligence*, Vol. 32.
- [18] Ninghao Liu, Qiaoyu Tan, Yuening Li, Hongxix Yang, Jingren Zhou, and Xia Hu. 2019. Is a single vector enough? exploring node polysemy for network embedding. In *Proceedings of the 25th ACM SIGKDD International Conference on Knowledge Discovery & Data Mining*. 932–940.
- [19] Qingsong Lv, Ming Ding, Qiang Liu, Yuxiang Chen, Wenzheng Feng, Siming He, Chang Zhou, Jianguo Jiang, Yuxiao Dong, and Jie Tang. 2021. Are we really making much progress? revisiting, benchmarking and refining heterogeneous graph neural networks. In *Proceedings of the 27th ACM SIGKDD conference on knowledge discovery & data mining*. 1150–1160.
- [20] Tomas Mikolov, Kai Chen, Greg Corrado, and Jeffrey Dean. 2013. Efficient estimation of word representations in vector space. *arXiv preprint arXiv:1301.3781* (2013).

- [21] Chanyoung Park, Carl Yang, Qi Zhu, Donghyun Kim, Hwanjo Yu, and Jiawei Han. 2020. Unsupervised differentiable multi-aspect network embedding. In *Proceedings of the 26th ACM SIGKDD International Conference on Knowledge Discovery & Data Mining*. 1435–1445.
- [22] Yundong Sun, Dongjie Zhu, Haiwen Du, and Zhaoshuo Tian. 2022. MHNF: Multi-hop Heterogeneous Neighborhood information Fusion graph representation learning. *arXiv:2106.09289 [cs.LG]*
- [23] Laurens Van der Maaten and Geoffrey Hinton. 2008. Visualizing data using t-SNE. *Journal of machine learning research* 9, 11 (2008).
- [24] Petar Veličković, Guillem Cucurull, Arantxa Casanova, Adriana Romero, Pietro Lio, Yoshua Bengio, et al. 2017. Graph attention networks. *stat* 1050, 20 (2017), 10–48550.
- [25] Xiao Wang, Houye Ji, Chuan Shi, Bai Wang, Yanfang Ye, Peng Cui, and Philip S Yu. 2019. Heterogeneous graph attention network. In *The world wide web conference*. 2022–2032.
- [26] Xiao Wang, Nian Liu, Hui Han, and Chuan Shi. 2021. Self-supervised heterogeneous graph neural network with co-contrastive learning. In *Proceedings of the 27th ACM SIGKDD conference on knowledge discovery & data mining*. 1726–1736.
- [27] S. Yun, M. Jeong, R. Kim, J. Kang, and H. J. Kim. 2019. Graph Transformer Networks. In *Advances in Neural Information Processing Systems*, Vol. 39. 1–12.

## Appendix

### A. Baselines Code and Datasets

MF2Vec is implemented using PyTorch. Table 9 lists the URLs of the authors' implementations of the compared methods, and Table 10 provides the URLs where the datasets can be downloaded.

**Table 9: Baseline URLs for Implemented Methods**

Method	URL
RGCN	<a href="https://github.com/BUPT-GAMMA/OpenHGNN">https://github.com/BUPT-GAMMA/OpenHGNN</a>
RGAT	<a href="https://github.com/BUPT-GAMMA/OpenHGNN">https://github.com/BUPT-GAMMA/OpenHGNN</a>
HGT	<a href="https://github.com/BUPT-GAMMA/OpenHGNN">https://github.com/BUPT-GAMMA/OpenHGNN</a>
HetSANN	<a href="https://github.com/BUPT-GAMMA/OpenHGNN">https://github.com/BUPT-GAMMA/OpenHGNN</a>
Simple-HGN	<a href="https://github.com/BUPT-GAMMA/OpenHGNN">https://github.com/BUPT-GAMMA/OpenHGNN</a>
MP2vec	<a href="https://github.com/BUPT-GAMMA/OpenHGNN">https://github.com/BUPT-GAMMA/OpenHGNN</a>
HAN	<a href="https://github.com/BUPT-GAMMA/OpenHGNN">https://github.com/BUPT-GAMMA/OpenHGNN</a>
MAGNN	<a href="https://github.com/cynricfu/MAGNN">https://github.com/cynricfu/MAGNN</a>
HeCo	<a href="https://github.com/liun-online/HeCo">https://github.com/liun-online/HeCo</a>
MHNF	<a href="https://github.com/BUPT-GAMMA/OpenHGNN">https://github.com/BUPT-GAMMA/OpenHGNN</a>
HGMAE	<a href="https://github.com/BUPT-GAMMA/OpenHGNN">https://github.com/BUPT-GAMMA/OpenHGNN</a>
HMSG	<a href="https://github.com/junxincuai/HMSG">https://github.com/junxincuai/HMSG</a>
MECCH	<a href="https://github.com/cynricfu/MECCH">https://github.com/cynricfu/MECCH</a>

**Table 10: Dataset URLs**

Dataset	URL
Yelp	<a href="https://github.com/librahu/HERec/tree/master/data">https://github.com/librahu/HERec/tree/master/data</a>
Movielens	<a href="https://github.com/librahu/HIN-Datasets-for-Recommendation-and-Network-Embedding">https://github.com/librahu/HIN-Datasets-for-Recommendation-and-Network-Embedding</a>
DBLP	<a href="https://github.com/liun-online/HeCo/tree/main/data/dblp">https://github.com/liun-online/HeCo/tree/main/data/dblp</a>
ACM	<a href="https://github.com/liun-online/HeCo/tree/main/data/acm">https://github.com/liun-online/HeCo/tree/main/data/acm</a>
IMDB	<a href="https://github.com/junxincuai/HMSG/tree/main/HMSG">https://github.com/junxincuai/HMSG/tree/main/HMSG</a>
Freebase	<a href="https://github.com/idirlab/freebases">https://github.com/idirlab/freebases</a>

### B. Baselines

We compare MF2Vec against state-of-the-art relation-based HGNNs and metapath-based HGNNs, categorized as follows:

#### Relation-Based HGNNs.

- RGCN: Introduces a relational graph convolutional network that assigns weights to each relation type, enabling the learning of structural information in heterogeneous graphs.
- RGAT: Applies attention mechanisms to each relation type in relational graphs, effectively integrating information in heterogeneous graphs.
- HGT: Utilizes a modified transformer architecture that considers various node and edge types in heterogeneous graphs to learn complex relationships.

- HetSANN: Applies attention mechanisms to learn structural information between nodes in heterogeneous graphs without relying on metapaths.
- Simple-HGN: Provides efficient and effective node embeddings in heterogeneous graphs through a simplified structure.

#### Metapath-Based HGNNs.

- MP2Vec: Proposes a node embedding technique in heterogeneous networks using metapaths to effectively capture diverse relationships.
- HAN: Develops a hierarchical attention mechanism-based model to learn the importance of nodes in heterogeneous graphs using metapaths.
- MAGNN: Enhances node embedding performance in heterogeneous graphs by leveraging intermediate node information within metapaths.
- HeCo: Combines self-supervised learning and contrastive learning in heterogeneous graphs to improve node representation learning performance.
- MHNF: A framework that automatically extracts metapaths in heterogeneous networks and utilizes them for node embedding learning.
- HGMAE: Utilizes masked autoencoders to learn robust node representations in heterogeneous graphs.
- HMSG: Integrates multi-scale structural information in heterogeneous graphs to enhance node representation learning performance.
- MECCH: Improves node embedding performance in heterogeneous graphs by leveraging contextual information of metapaths.

### C. Stability of Performance Across Metapaths

Tables 11, 12, and 13 present performance metrics for the top three models and MF2Vec across the DBLP, ACM, and IMDB datasets, respectively, based on a single metapath. Across all datasets, MF2Vec consistently outperforms other models, achieving the highest Mi-F1, Ma-F1, and AUC scores for all metapaths. On the DBLP dataset (Table 11), MF2Vec excels across all metrics. Similarly, on the ACM dataset (Table 12), it achieves the best performance for both PAP and PSP metapaths. On the IMDB dataset (Table 13), MF2Vec again demonstrates its robustness and consistency, achieving the highest scores across all metapaths.

**Table 11: Performance in DBLP based on a single metapath for the top 3 models and MF2Vec. Best results are highlighted in bold and the second-best results are underlined.**

Metapath	DBLP			DBLP		
Metric	APTPA	APCPA	APA	ALL		
Metric	Mi-F1	Ma-F1	AUC	Mi-F1	Ma-F1	AUC
MAGNN	0.670	0.685	0.912	0.918	0.925	0.988
HMSG	0.604	0.498	0.843	0.889	0.887	0.990
MECCH	0.825	0.819	0.946	0.936	0.933	0.993
MF2Vec	<b>0.904</b>	<b>0.907</b>	<b>0.986</b>	<b>0.958</b>	<b>0.956</b>	<b>0.990</b>
				<u>0.667</u>	<u>0.670</u>	<u>0.861</u>
				0.963	0.962	0.995

**Table 12: Performance in ACM based on a single metapath for the top 3 models and MF2Vec. Best results are highlighted in bold and the second-best results are underlined.**

Metapath	ACM					
	PAP			PSP		
Metric	Mi-F1	Ma-F1	AUC	Mi-F1	Ma-F1	AUC
MAGNN	0.6064	0.6602	<u>0.8754</u>	0.7298	<b>0.7649</b>	<u>0.8575</u>
HMSG	0.6608	0.6024	0.8598	<u>0.7656</u>	0.7128	0.8302
MECCH	<u>0.6683</u>	0.6405	0.8431	0.7531	0.7067	<u>0.8440</u>
MF2Vec	<u>0.8080</u>	0.8013	<u>0.9322</u>	0.7631	0.7211	0.8436

**Table 13: Performance in IMDB based on a single metapath for the top 3 models and MF2Vec. Best results are highlighted in bold and the second-best results are underlined.**

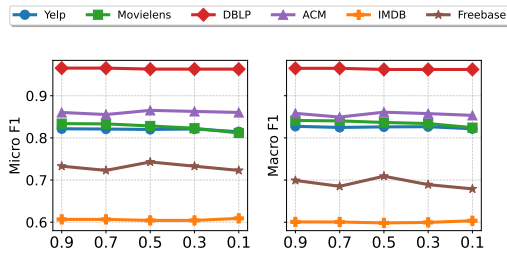
Metapath	IMDB		
	MAM		
Metric	Mi-F1	Ma-F1	AUC
MAGNN	0.5241	0.5276	0.7072
HMSG	0.4717	0.4587	0.6213
MECCH	0.4149	0.3169	0.5887
MF2Vec	<u>0.5875</u>	<u>0.5733</u>	<b>0.7180</b>

Metapath	MDM		
	ALL		
Metric	Mi-F1	Ma-F1	AUC
MAGNN	0.5057	0.5180	0.6971
HMSG	0.4226	0.3634	0.5554
MECCH	0.4029	0.3601	0.5603
MF2Vec	<u>0.5851</u>	<u>0.5565</u>	<u>0.7142</u>

We evaluate the performance of these models across three downstream tasks: node classification, link prediction, and node clustering.

## D. Ablation Study



**Figure 10: Performance of MF2Vec on six datasets with varying Temperature ( $\tau$ )**

**D.1. Effect of Temperature ( $\tau$ ).** From Figure 10, we observe the sensitivity of the Gumbel-Softmax in calculating the probability across all classes with varying  $\tau$ . According to the performance metrics, the model's performance exhibits minor variations in MovieLens, DBLP, and Yelp, and changes within a 2% range in MovieLens and Freebase. The results indicate that the sensitivity of the model to different values of  $\tau$  is relatively stable across datasets, with minor fluctuations in the Macro F1 and Micro F1 scores.

**D.2. Graph Method.** Table 14 compares GCN, EdgeGAT, and GraphSAGE to evaluate the impact of facet features as edge weights. GCN outperforms across all datasets, achieving AUC and F1 scores above 0.99 on DBLP and ACM by effectively leveraging edge weights to capture local and global relationships. While EdgeGAT models relationship importance using attention, its performance is less consistent, and GraphSAGE shows lower results due to its limited capacity to represent multi-facet relationships despite its efficiency. These findings highlight the significance of edge weights in facet-based graph learning.

## F. Algorithms for Random Walk and Sub-graph Generation

This section describes the algorithms used for random walk and sub-graph generation in heterogeneous networks. The random walk algorithm explores paths within the graph, while the sub-graph generation algorithm utilizes these paths to construct sub-graphs based on specific node types.

**F.1. Random Walk Algorithm.** The first algorithm 2 performs a random walk on a network. It generates a path of a specified length starting from a given node. The path is built by selecting a random neighbor at each step. If a neighbor cannot be found or if the end node of the path does not match the desired node type, the algorithm returns None.

### Algorithm 2 Random Walk

```

Input: Network  $G = (V, \mathcal{E})$ , node types  $V'$ , start node  $v_i \in V'$ , path length  $pathLength$ 
Output: A path  $path(v_i, v_j)$  or None
Initialize:  $path = [v_i]$ 
for  $step = 0$  to  $pathLength - 1$  do
     $v_m \leftarrow path[-1]$ 
     $v_{m+1} \leftarrow neighbors(G, v_m)$ 
    if  $v_{m+1}$  does not exist then
        return None
    else
        Append  $v_{m+1}$  to  $path$ 
    end if
end for
 $v_j \leftarrow path[-1]$ 
if  $v_j \in V'$  then
    return  $path(v_i, v_j)$ 
else
    return None
end if

```

**F.2. Sub-graph Generation Using Random Walk Paths.** The second algorithm 3 generates a sub-graph from the network using multiple random walks. For each node, several random walks are performed to collect paths. Unique node pairs are recorded to avoid duplicates. The sub-graph is constructed by adding nodes and edges based on the collected paths.

### Algorithm 3 Sub-graph Generation Using Random Walk Paths

```

Input: Network  $G = (V, \mathcal{E})$ , node types  $V'$ , start node  $v_i \in V'$ , path length  $pathLength$ , attempts  $attempts$ 
Output: Sub-graph  $G' = (V', \mathcal{E}')$ 
Initialize:  $paths = []$ ,  $pairs = []$ 
for each node  $v_i \in V'$  do
    for attempt = 0 to  $attempts - 1$  do
         $path(v_i, v_j) \leftarrow RANDOM\_WALK(G, v_i, V', pathLength)$ 
        if  $(path[0], path[-1]) \notin pairs$  then
            Append  $(path[0], path[-1])$  to  $pairs$ 
            Append  $path(v_i, v_j)$  to  $paths$ 
        end if
    end for
end for
Extract nodes  $(v_i, v_j, v_s)$  from  $paths$ 
Create sub-graph  $G'$  by adding nodes from  $dgl.graph(v_i, v_j)$ 
Add edges  $v_s$  to  $G'(E')$ 
return  $G'$ 

```

**Table 14: Performance comparison of different models (GCN (Ours), Edge GAT, and GraphSAGE) across Yelp, MovieLens, DBLP, ACM, IMDB, and Freebase datasets. The best results are highlighted in bold and the second-best results are underlined.**

Model	Yelp			MovieLens			DBLP			ACM			IMDB			Freebase		
	AUC	Mi-F1	Ma-F1															
GCN (Ours)	<b>0.8947</b>	<b>0.8200</b>	<b>0.8261</b>	<u>0.9074</u>	<u>0.8283</u>	<u>0.8366</u>	<b>0.9958</b>	<b>0.9631</b>	<b>0.9623</b>	<b>0.9528</b>	<b>0.8653</b>	<b>0.8610</b>	<b>0.7709</b>	<b>0.6211</b>	<b>0.6117</b>	<b>0.8701</b>	<b>0.7429</b>	<b>0.6991</b>
Edge GAT	0.8624	0.8041	0.7941	0.8629	0.8086	0.8180	0.990±0.002	0.928±0.007	0.921±0.007	0.950±0.005	0.854±0.008	0.849±0.010	0.745±0.013	0.579±0.023	0.558±0.025	0.795±0.010	0.681±0.010	0.614±0.026
GraphSAGE	0.8296	0.7701	0.7771	0.8028	0.7506	0.7719	0.983±0.005	0.902±0.020	0.896±0.022	0.938±0.006	0.816±0.009	0.809±0.009	0.702±0.018	0.531±0.029	0.501±0.031	0.734±0.018	0.640±0.021	0.471±0.016